JAAS

PAPER

View Article Online
View Journal | View Issue

Cite this: J. Anal. At. Spectrom., 2018, 33, 2116

Emission enhancement of laser-induced breakdown spectroscopy by increasing sample temperature combined with spatial confinement

Jin Guo,[a] Tingfeng Wang,[a] Junfeng Shao,[a] Anmin Chen *[bc] and Mingxing Jin*[bc]

Received 23rd July 2018
Accepted 8th October 2018

DOI: 10.1039/c8ja00246k

rsc.li/jaas

To enhance spectral intensity in laser-induced breakdown spectroscopy, increasing the sample temperature and spatial confinement were used simultaneously to improve optical emission of plasmas induced from silicon target using a Nd:YAG laser pulse in air. The sample was uniformly heated to temperatures ranging from a low temperature (25 °C) to a high temperature (250 °C) with laser energy of 60 mJ, and a cylindrical cavity with a diameter of 6 mm and a depth of 6 mm was used to confine the plasma. The results illustrated that as the sample temperature increased, the spectral intensity of plasma without spatial confinement appeared to saturate at a sample temperature of 150 °C. When the cylindrical cavity was present, the spectral intensity increased monotonically along with the sample temperature. The enhancement effect of combining spatial confinement and increasing the sample temperature was stronger than that of spatial confinement or increasing the sample temperature alone. The experimental results indicated that the optical emission intensity can be further improved by combining the two enhancement effects.

1. Introduction

After the invention of the laser in 1960, the first useful laser-induced plasma (LIP) was demonstrated by a ruby laser on a surface.[1] More and more attention of researchers has been paid to LIP.[2–5] Over the past few decades, LIP has developed rapidly as an analytical technique, including laser-induced breakdown spectroscopy (LIBS) and laser-induced plasma spectroscopy.[6] LIBS can use distinct characteristic spectral lines emitted from LIP to determine the elements within a sample. LIBS can be used to analyze any matter, regardless of its physical state: rocks, glasses, metals, sand, teeth, bones, weapons, powders, hazards, liquids, plants, biological material, polymers, *etc.* LIBS can be performed at atmospheric pressure, in a vacuum, at the depths of the ocean, or in space exploration.[7] In these applications of LIBS, it is critical to enhance the plasma and thus to increase the plasma emission intensity and the signal-to-noise ratio.[8] There have been a number of different techniques proposed for doing so, such as spark discharge-assisted LIBS,[9–11] spatially confined LIBS,[12–14] magnetic field-enhanced LIBS,[15,16] LIBS with preheated sample,[17–20] flame-enhanced LIBS,[21,22] resonance-enhanced LIBS,[23,24] nanoparticle-enhanced LIBS,[25,26] and double-pulse LIBS.[27–29]

In addition, to further improve the LIBS performance, the combination of two techniques mentioned above is used to enhance the emission intensity in LIP. Hou *et al.* investigated the combination of cylindrical confinement and spark discharge for signal improvement in LIBS.[30] These two methods were combined together not only to improve the pulse-to-pulse signal repeatability but also to simultaneously and significantly enhance the signal as well as signal-to-noise ratio. Guo *et al.* studied the enhancement of optical emission in LIBS,[31] both a pair of permanent magnets and an aluminum hemispherical cavity (diameter: 11.1 mm) being used simultaneously to magnetically and spatially confine plasmas produced by a KrF excimer laser in air from pure metal and alloyed samples. High enhancement factors of about 22 and 24 in the emission intensity of Co and Cr lines were acquired using the combined confinement, while enhancement factors of only about 11 and 12 were obtained just with a cavity. They also studied enhanced optical emission in LIBS by combining spatial confinement and dual-pulse irradiation.[32] A significant enhancement factor of 168.6 for the emission intensity of Cr lines was obtained using the combined spatial confinement and DP-LIBS, as compared with an enhancement factor of 106.1 with DP-LIBS only. Hao *et al.* investigated the improvement of the detection sensitivity of vanadium (V) and manganese (Mn) elements in steel using LIBS.[33] A ring magnet was employed to spatially and magnetically confine plasmas produced from steel samples using an Nd:YAG laser. The results showed that the optical emission and

[a]State Key Laboratory of Laser Interaction with Matter, Innovation Laboratory of Electro-Optical Countermeasures Technology, Changchun Institute of Optics, Fine Mechanics and Physics, Chinese Academy of Sciences, Changchun 130033, China
[b]Institute of Atomic and Molecular Physics, Jilin University, Changchun 130012, China. E-mail: amchen@jlu.edu.cn; mxjin@jlu.edu.cn
[c]Jilin Provincial Key Laboratory of Applied Atomic and Molecular Spectroscopy (Jilin University), Changchun 130012, China

signal-to-noise ratios for both V(I) 437.92 nm and Mn(I) 403.08 nm lines were enhanced by the ring-magnet confinement. Hussain *et al.* investigated the combined effects of double pulses and magnetic field on emission enhancement of LIBS from aluminum plasma.[34] Enhancement factors of about 11 and 5 were obtained in DP-LIBS with and without magnetic field, respectively. The effect of inter-pulse delay time on the intensity enhancement shows a maximum enhancement factor of about 70 and 40 in DP-LIBS with and without magnetic field for atomic line (Al 308.2 nm). Su *et al.* discussed the optical emission character of dual-pulse laser plasma with cylindrical cavity confinement.[35] Two collinear pulse laser beams and a cylindrical cavity are combined together to generate and confine the laser plasma and are used to evaluate the performance of the confined collinear dual-pulse LIBS. The optical emission characters of the confined plasmas, as well as the temperature and electron number density of the plasma were carefully investigated. Khalil developed the double-pulse laser ablation technique to generate gold (Au) plasma and produce high current with application of an electric potential in an argon ambient gas environment.[36] The results indicated that the velocity distribution function and current signals depend on the applied discharge voltage, laser intensity, laser wavelength and ambient argon gas pressure. A seven-fold increase in the current signal was achieved by increasing the applied discharge voltage and ion velocity under application of a double-pulse laser field.

In view of the above discussion, the combination of two techniques can further improve the spectral intensity of LIBS. However, no direct study has been performed to date on the combined effect of laser-induced preheating of the sample with cavity confinement.[14,19] For spatial confinement, the mechanism of spectral enhancement is based on the compression of the plasma plume with the shock wave reflected by the wall of the spatial confinement cavity.[13,32,33,35,37] The particle number density in the plasma plume increases, and the corresponding probability of collision between particles within the plasma increases. This results in an increase in optical emission of plasma. For the preheated sample, the sample temperature can change the coupling between laser and plasma, the density and pressure of ambient gas, and the characteristic parameters (integral intensity, plume area) of the plasma plume.[17,18,20,38] When the two techniques are combined together, the reflected shock wave in spatial confinement will compress the plasma plume of the laser-induced preheated sample. The corresponding results will be expected to be more interesting.

In this paper, our aim was to further improve the enhancement effects by increasing the sample temperature and the spatial confinement. These two methods were combined together to generate and confine laser plasma. The effects of combining spatial confinement and increasing the sample temperature were investigated comparing with spatial confinement or increasing the sample temperature alone. The experimental results indicated that the optical emission intensity was further improved by combining the two enhancement effects.

2. Experimental setup

The experimental setup of laser-induced Si plasma used for investigating the effects of the combination of spatial confinement and increasing the sample temperature on LIBS is presented in Fig. 1. A Q-switch Nd:YAG laser system (Continuum, Surelite III) was used to excite the target to produce the plasma. The repetition rate was 10 Hz with a wavelength of 1064 nm. The full width at half maximum of the pulse was 10 ns. A planoconvex lens with 10 cm focal length of 25 mm in diameter was used to focus the nanosecond laser pulse onto the silicon (Si⟨100⟩) surface. The focal point of the focusing lens was 5 mm under the target surface to avoid air breakdown. The silicon target was attached on the surface of a heating element by using thermal grease compound. A thermocouple and an electric heating resistor were the main components of the heating element. The thermocouple was used to monitor the temperature and the electric heating resistor was used to heat the sample. In the process of heating, when the temperature reached the desired value, the thermocouple monitored the temperature and sent feedback to the heating resistor, which stopped heating. If the temperature dropped, the heating resistor continued to raise the temperature. In addition, a cylindrical cavity with a diameter of 6 mm and a depth of 6 mm was placed tightly on the surface of the silicon target surface. The silicon plasma was produced inside the cylindrical cavity, and was located at the center of cylindrical cavity. To avoid over-ablation, the silicon target and the heating element were mounted on a computer-controlled three-dimensional stage (Thorlabs China, PT3/Z8M) to provide a fresh target. The emission light from the laser-excited silicon plasma was collected by the planoconvex focusing lens. A dichroic mirror (DM) and another planoconvex lens (BK7, 75 cm focal length, 50 mm diameter) were used to focus the collected light into a fiber. This optical fiber was coupled to a spectrometer (SP 500I, 1200 grooves per mm, Princeton Instruments, Acton). The spectrum dispersed by the spectrometer was detected by using an ICCD (intensified charge-coupled device, Princeton Instruments, PIMAX4, 1024 × 1024 pixels). The delay time between

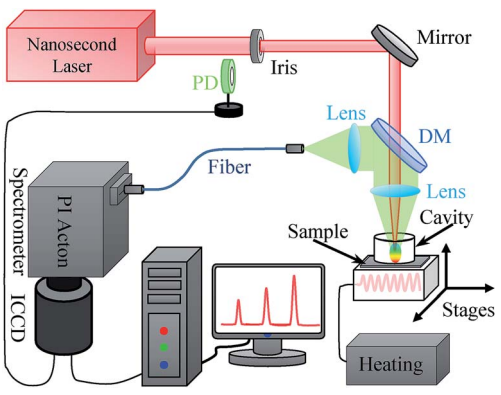

Fig. 1 Experimental setup of spatially confined laser-induced silicon plasmas with different sample temperatures (DM, dichroic mirror; PD, photodiode).

the ICCD and laser pulse was synchronized by using a photodiode. The signal of the photodiode came from scattered light at the output window of the laser system. And, the signal of the photodiode was considered as the zero reference time point of the whole experimental system. The obtained spectra were averaged over 20 laser pulses. The experiment was performed in air.

3. Results and discussion

First of all, to study the combination of sample preheating effect and spatial confinement effect in LIBS, a comparison was performed among the optical emission obtained at 25 °C, at 250 °C, and at 250 °C with spatial confinement. Fig. 2 shows the spectral emission of Si(I) line at 390.55 nm from the $3s^23p^2(^1S_0) \leftarrow 3s^22p4s(^1P_1)$ transition for different sample temperatures (25 °C and 250 °C) and with spatial confinement. As seen from Fig. 2, for the Si(I) line, plasma emission intensity at high temperature (250 °C) was stronger than that at low temperature (25 °C). When the spectral line was measured at the higher sample temperature (250 °C) with spatial confinement, the emission intensity was much stronger. And, with the change of experimental conditions (increasing sample temperature and spatial confinement), the emission intensity of the spectral line increased, while the spectral baseline intensity remained almost unchanged.

3.1 Spatial confinement effect

The time-resolved optical emission spectra of the laser-induced silicon plasmas in a spectral range from 390 nm to 391 nm were measured to demonstrate the spectral emission enhancement effect with and without the cylindrical confining cavity, as shown in Fig. 3. The measured spectral line was Si(I) at 390.55 nm. As seen from Fig. 3(a), the emission intensity of the Si(I) line in the absence of the cylindrical cavity decayed monotonically with the increase of delay time. However, when the silicon plasma was produced inside the cylindrical cavity, the emission intensity of the Si(I) line was improved in the range of the delay time from 5 μs to 12 μs. In order to better compare the increase in the spectral line intensity, we selected a typical

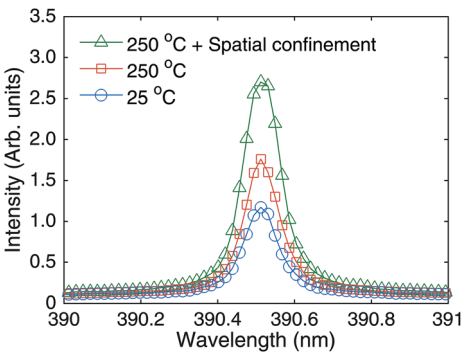

Fig. 2 Comparison of Si(I) line at 390.55 nm under different experimental conditions. Delay time is 5 μs. Gate width is 0.5 μs. Laser energy is 60 mJ.

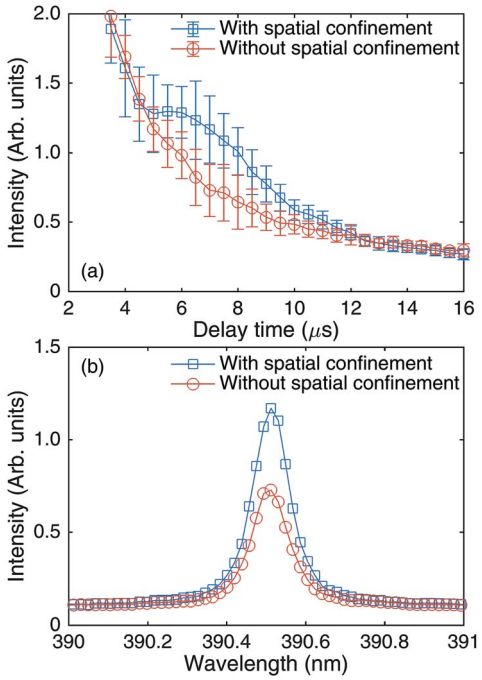

Fig. 3 (a) Time-resolved spectroscopy of Si(I) line at 390.55 nm with (square) and without (circle) the cylindrical cavity. (b) Comparison of spectral lines with (square) and without (circle) the cylindrical cavity at 7 μs delay time. Gate width is 0.5 μs. Laser energy is 60 mJ.

delay time (7 μs) from Fig. 3(a). As shown in Fig. 3(b), the emission intensity of the Si(I) line was enhanced obviously in the case of spatial confinement, the enhanced factor being approximately 2. Compared with the case in the absence of the cylindrical cavity, there was almost no increase in the baseline intensity of the spectrum with spatial confinement. Meanwhile, the signal-to-background ratio was also improved. In this period, the plasma emitted sharp atomic spectral lines with a low background (continuous spectrum) and highly favorable characteristics for elemental analysis. When the target was excited to produce the plasma in ambient gas, the plasma was accompanied by a shock wave (shock wave can be observed by using Schlieren, interferometry and shadowgraphy).[39,40] The velocity of the shock wave was greater than that of the plasma plume. For spatially confined LIP, during the expansion of the shock wave, the shock wave encountered the wall of the cylindrical cavity, and it could be reflected, and propagated to the plasma plume.[39,41] The shock wave compressed the plasma plume into a smaller size,[37,40] and then the probability of collision between particles within the plasma increased, resulting in an increase in optical emission intensity.

3.2 Sample temperature effect

Sample temperature plays an important role in the laser-target interaction in LIBS. Increasing the sample temperature is another effective physical condition for the enhancement of spectral intensity for LIBS. Fig. 4 illustrates the spectral emission of laser-induced Si plasmas at two sample temperatures (25 °C and 250 °C). The corresponding spectral line is Si(I) at

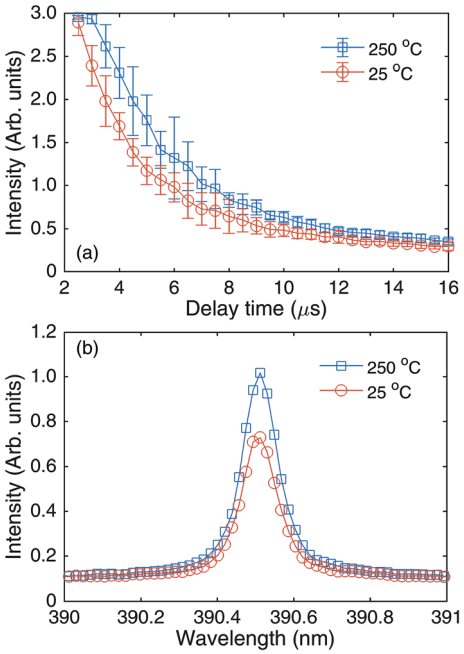

Fig. 4 (a) Time-resolved spectroscopy of Si(I) line at 390.55 nm at sample temperatures of 25 °C (circle) and 250 °C (square). (b) Comparison of spectral lines at sample temperatures of 25 °C (circle) and 250 °C (square) for delay time of 7 μs. Gate width is 0.5 μs. Laser energy is 60 mJ.

390.55 nm. Fig. 4(a) presents the evolution of the peak intensity of Si(I) at 390.55 nm with increasing delay time. The spectral intensity decreased monotonically. Also, the spectral line intensity was sensitive to the sample temperature; the spectral intensity at a sample temperature of 25 °C was higher than that at a sample temperature of 250 °C. Fig. 4(b) compares the spectra at sample temperatures of 25 °C and 250 °C. It is noted that increasing the sample temperature distinctly enhanced the spectral intensity; this was an approximately 1.5-fold enhancement when the sample temperature increased from 25 °C to 250 °C. This result shows that heating the sample can enhance the spectral line intensity. The enhancement of the spectral line by increasing the target temperature is based on two main mechanisms. One is that more target material is excited from the target surface by enhancing the laser-target interaction due to reduced optical reflectivity on the target surface.[18,19,42] The other is that the enhanced effect is attributed to the expansion dynamics of the LIP plume; the hydrodynamic effect produced by heating the air around the target surface improves the plasma plume expansion.[17,38,43] In particular, the size of the plasma plume at a higher sample temperature is larger than that at lower sample temperatures for the same laser energy. A higher sample temperature facilitated plume expansion in air. Increasing the sample temperature will lead to a significant change in the structure of the plasma plume. Moreover, the spatial confinement conditions have a significant influence on the morphology of the plasma plume and the enhancement of the emission intensity.[37] The enhancement will be more obvious when the generated shock wave compresses the larger size plasma plume. To better understand the combined influence of these two methods, corresponding LIBS results in air are discussed below.

3.3 Combination of two effects

Fig. 5 shows the temporal evolution of the emission intensity from the Si(I) 390.55 nm peak as functions of the delay time at 25 °C sample temperature without spatial confinement, at 250 °C sample temperature without spatial confinement, at 25 °C sample temperature with spatial confinement, and at 250 °C sample temperature with spatial confinement. The Si(I) line was significantly enhanced when both the cylindrical cavity and increased sample temperature were used. The emission intensity enhancement was different with different delay times from 3 μs to 11 μs. When the cylindrical cavity was used to confine the plasma generated by different laser-induced sample temperatures, two significant enhancement peaks were observed. For 25 °C sample temperature, the emission enhancement occurred during the time periods from 5 to 11 μs, while the emission enhancement occurred from 3.5 to 10 μs as the sample was heated to 250 °C. The encounter time between the reflected shock wave and the generated plasma plume was early for the case with higher sample temperature, and the emission enhancement became more obvious. As mentioned above, on the one hand, the increase in the sample temperature can enhance the coupling between laser and target, producing a stronger shock wave; on the other hand, increasing the sample temperature improves the size of the plasma plume including lateral and axial directions. For the spatial confinement effect, two main factors are the shock wave and plasma plume. Therefore, when the sample was heated to a higher temperature, this led to a larger size plasma plume; meanwhile, the stronger shock wave compressed the larger size plasma plume resulting in the stronger optical emission. And, the expansion

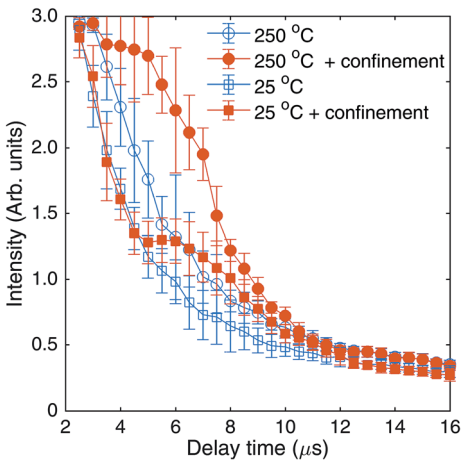

Fig. 5 Time-resolved spectroscopy of Si(I) line at 390.55 nm at 25 °C sample temperature without spatial confinement (open square), at 250 °C sample temperature without spatial confinement (open circle), at 25 °C sample temperature with spatial confinement (solid square), and at 250 °C sample temperature with spatial confinement (solid circle). Gate width is 0.5 μs. Laser energy is 60 mJ.

velocities of shock wave and plasma plume were faster compared with the case at the lower sample temperature so that the traveling time between the shock wave and the plasma plume was shorter. Subsequently, the combined effect of target temperature and spatial confinement on the emission line of plasma produced from LIBS in the atmosphere is discussed in detail.

Fig. 6 illustrates the evolutions of the Si(I) emission intensity as functions of the time delay at different sample temperatures without spatial confinement and at different sample temperatures with spatial confinement. As seen in Fig. 6(a), from 25 °C to 150 °C, increasing the sample temperature improved the spectral line intensities for different delay times. In the range of temperature from 150 °C to 250 °C, the spectral intensity was almost equal for each temperature, and a saturation phenomenon appeared. However, it is observed that the emission intensities were continuously enhanced when the cylindrical cavity was used to confine the plasma plumes at different sample temperatures; see Fig. 6(b). The influence of the spatial confinement with different sample temperatures on the enhancement of emission intensity was further analyzed, as shown in Fig. 7. We performed statistical analysis on the enhancement ratio calculated by dividing the results of Fig. 6(b) by those of Fig. 6(a). From this figure, the encounter time between shock wave and plasma plume shortened from 5 μs to 3.5 μs. This revealed that the velocity of the shock wave became faster as the sample temperature increased. The maximum enhancement ratio also increased from 1.5 to 1.9, suggesting that the interaction of shock wave and plasma plume became stronger.

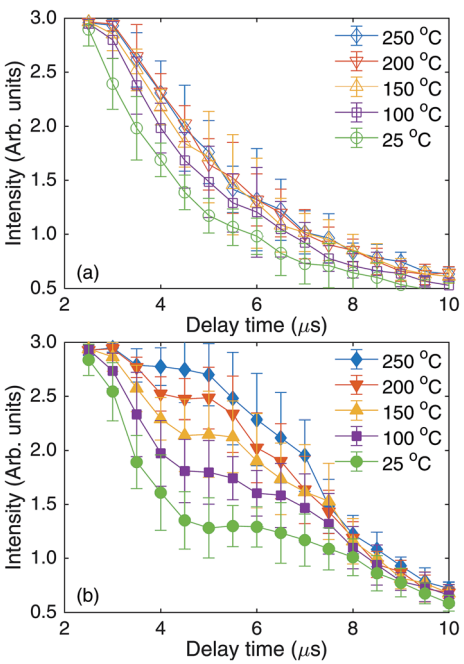

Fig. 6 Time-resolved spectroscopy of Si(I) line at 390.55 nm at different sample temperatures without spatial confinement (a) and at different sample temperatures with spatial confinement (b). Gate width is 0.5 μs. Laser energy is 60 mJ.

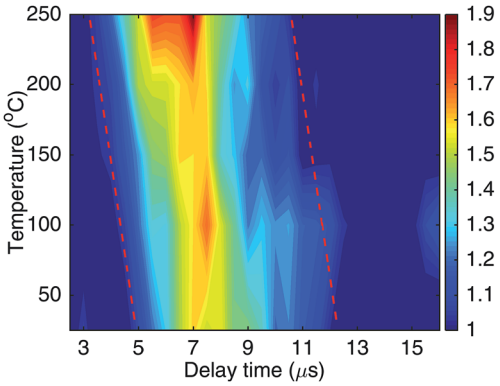

Fig. 7 Distribution of enhancement ratio along with delay time and sample temperature. The ratio is calculated by dividing the results of Fig. 6(b) by those of Fig. 6(a).

To better understand the influence of the combination of sample temperature and spatial confinement, the corresponding LIBS results in air are discussed below. Fig. 8 selected from Fig. 6 shows the evolutions of the emission intensity as functions of the sample temperature without spatial confinement and with spatial confinement for different delay times (5 μs and 6 μs). In Fig. 8, at the beginning of increasing the sample temperature, the spectral intensity visibly increased at two different delay times for the case without spatial confinement. With an increase in the sample temperature, the spectral

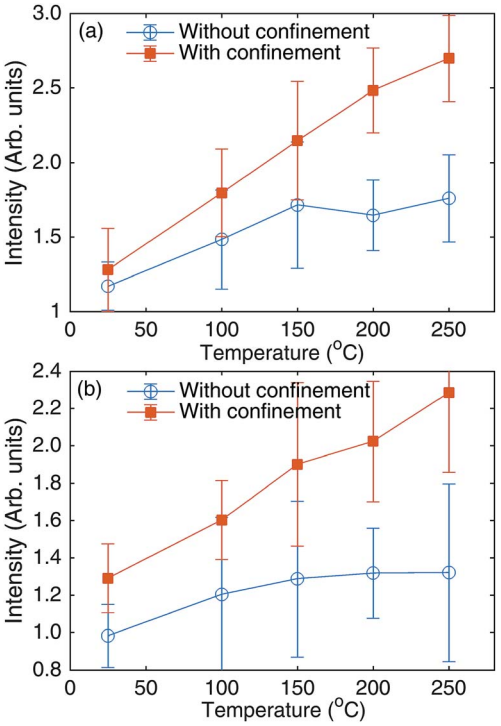

Fig. 8 Evolution of intensity of Si(I) line at 390.55 nm with the target temperature without spatial confinement and with spatial confinement for 5 μs (a) and 6 μs (b) delay times. Gate width is 0.5 μs. Laser energy is 60 mJ.

intensity reached a maximum at a sample temperature of 150 °C, and the increasing trend of the spectrum was no longer apparent. At sample temperatures below 150 °C, the slope of the curve was more significant compared to the trend of the whole graph. As mentioned above, an increase in the sample temperature is equivalent to an increase in absorbed laser energy. The saturation at higher sample temperature is expected to be attributable to the shielding effect (usually, researchers call it the plasma shielding effect),[44–47] *i.e.*, absorption and/or reflection of the laser photons by the plasma itself. When the target surface is irradiated by a laser beam, a high-temperature and high-density plasma is generated on the target surface. Next, the plasma plume rapidly expands, and the plasma will continue to absorb the laser energy in the processes of the expansion. Finally, the expanding plasma can prevent the laser reaching the target surface, resulting in the shielding effect. Haq *et al.* investigated the variation in emission intensities of magnesium plasmas as a function of laser irradiance.[48] The results showed an increasing trend with an increase of laser energy, and thereafter, the signal intensities started saturating due to the plasma shielding. Therefore, after the sample was heated to 150 °C, the plasma would suffer a strong plasma shielding effect, which leads to a saturation in LIBS signals (see Fig. 8).

However, when the cylindrical cavity was present, the spectral intensity increased monotonically along with the sample temperature in Fig. 8. Specifically, in the range of sample temperature from 150 °C to 250 °C, the spectral intensity without spatial confinement was almost constant, while the spectral intensity with spatial confinement increased continuously. Along with the sample temperature, increasing the temperature enhanced the coupling of laser and target. The stronger coupling generated a stronger shock wave, leading to a stronger compression on the plasma plume. At the sample temperature of 150 °C, a stronger plasma shielding effect occurred; although the absorbed laser energy of the target did not increase, the plasma could absorb more laser energy due to plasma shielding effect mentioned above. More laser energy was transferred to the shock wave.[49–51] The laser-supported shock wave would compress the plasma plume more effectively. The plasma plume was compressed even further than for the case at lower sample temperatures. The plasma density was drastically increased, which led to an increase in the collision probability among particles within the plasma. This enhanced collision in turn increased the number of excited atoms.[13,14,37] Therefore, the spectral intensities of the plasmas with the combination of spatial confinement and increasing sample temperature were further improved.

The relative standard deviation (RSD) is widely used in analytical chemistry to express the precision and repeatability of an assay. Researchers are often concerned about the problem of precision and repeatability. The repeatability in LIBS is very important for wide commercialization.[52] Fig. 9 shows the RSD at a delay time of 6 μs. For different sample temperatures, the RSD with spatial confinement was always lower than that without spatial confinement, while the influence of sample temperature was not obvious. The effect of spatial confinement on RSD

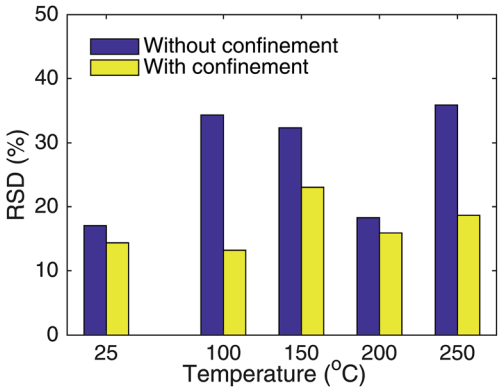

Fig. 9 Comparison of relative standard deviation (RSD) of spectral intensity without spatial confinement and with spatial confinement for different sample temperatures at 6 μs delay time.

mentioned by many researchers was an effective method to improve the RSD.[53,54]

Fig. 10(a) shows the distribution of the enhancement ratio of higher sample temperature and 25 °C sample temperature. With an increase of the sample temperature, the enhancement ratio in the delay time range from 4 μs to 8 μs presented a maximum. The maximum ratio was approximately 1.5. For all delay times, the ratio reached saturation as the sample was heated to 150 °C. Fig. 10(b) shows the distribution of the

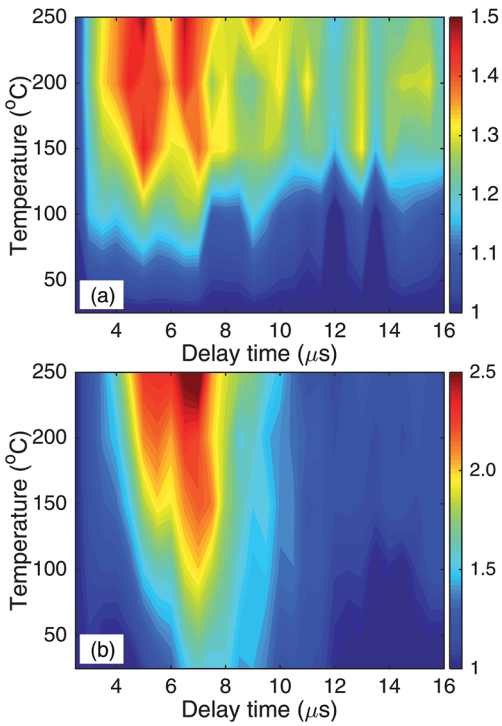

Fig. 10 (a) Distribution of enhancement ratio of higher sample temperature and 25 °C sample temperature. (b) Distribution of enhancement ratio of higher sample temperature with spatial confinement and 25 °C sample temperature without spatial confinement.

enhancement ratio of higher sample temperature with spatial confinement and 25 °C sample temperature without spatial confinement. For different delay times, the ratio increased continuously along with the sample temperature. For a delay time from 6 μs to 8 μs, the enhancement was stronger. The maximum ratio was approximately 2.5 at a sample temperature of 250 °C and delay time of 6.5 μs. As discussed above, when using the preheated sample alone, the optical emission of plasma would appear to saturate due to the plasma shielding effect. In contrast, spatial confinement using the cavity was not affected by plasma shielding, and could further improve the optical emission intensity. Therefore, spatial confinement will become more prominent and necessary for LIBS with a preheated sample.

4. Conclusions

In summary, the optical emission in a laser-induced preheated sample combined with spatial confinement was investigated by optical emission spectroscopy. A significant enhancement in the Si(I) 390.55 nm line from silicon plasma was observed. The results illustrated that the spectral intensity increased with sample temperature; at a sample temperature of 150 °C, the spectral intensity was saturated. The increase in the spectral intensity was attributed to the enhanced interaction between laser and sample, and the saturation of spectral intensity at higher sample temperature is based on the plasma shielding effect. When a cylindrical cavity was used to confine the plasma at higher sample temperature, the spectral intensity increased monotonically. The enhanced interaction between laser and sample generated a stronger shock wave. The stronger shock wave on the compression of the plasma plume was more effective, resulting in the higher optical emission. Also, the spatial confinement using the cavity was not affected by plasma shielding. It is obvious that the combined enhancement effects of increasing the sample temperature and spatial confinement are much stronger than those of spatial confinement or increasing the sample temperature alone. The results of this study provide further emission enhancement in the spectral line of LIBS.

Conflicts of interest

There are no conflicts to declare.

Acknowledgements

We acknowledge the support by the National Natural Science Foundation of China (grant no. 11674128, 11504129, and 11474129); Jilin Province Scientific and Technological Development Program, China (grant no. 20170101063JC); and the Fundamental Research Project of Chinese State Key Laboratory of Laser Interaction with Matter (grant no. SKLLIM1605).

References

1 F. Brech and L. Cross, *Appl. Spectrosc.*, 1962, **16**, 59–64.
2 Z.-Z. Wang, Y. Deguchi, Z.-Z. Zhang, Z. Wang, X.-Y. Zeng and J.-J. Yan, *Front. Phys.*, 2016, **11**, 114213.
3 Z. Wang, F. Dong and W. Zhou, *Plasma Sci. Technol.*, 2015, **17**, 617.
4 Z. Wang, T.-B. Yuan, Z.-Y. Hou, W.-D. Zhou, J.-D. Lu, H.-B. Ding and X.-Y. Zeng, *Front. Phys.*, 2014, **9**, 419–438.
5 L.-B. Guo, X.-Y. Li, W. Xiong, X.-Y. Zeng and Y.-F. Lu, *Front. Phys.*, 2016, **11**, 115208.
6 O. T. Butler, J. M. Cook, C. F. Harrington, S. J. Hill, J. Rieuwerts and D. L. Miles, *J. Anal. At. Spectrom.*, 2006, **21**, 217–243.
7 A. W. Miziolek, V. Palleschi and I. Schechter, *Laser induced breakdown spectroscopy*, Cambridge University Press. 2006.
8 X. Zhao and Y. C. Shin, *Appl. Phys. B: Lasers Opt.*, 2015, **120**, 81–87.
9 W. Zhou, X. Su, H. Qian, K. Li, X. Li, Y. Yu and Z. Ren, *J. Anal. At. Spectrom.*, 2013, **28**, 702–710.
10 W. Zhou, K. Li, Q. Shen, Q. Chen and J. Long, *Opt. Express*, 2010, **18**, 2573–2578.
11 K. Li, W. Zhou, Q. Shen, J. Shao and H. Qian, *Spectrochim. Acta, Part B*, 2010, **65**, 420–424.
12 X. Shen, J. Sun, H. Ling and Y. Lu, *J. Appl. Phys.*, 2007, **102**, 093301.
13 Y. Wang, A. Chen, L. Sui, S. Li, X. Wang, Y. Jiang, X. Huang and M. Jin, *J. Anal. At. Spectrom.*, 2016, **31**, 1974–1977.
14 X. Wang, A. Chen, Y. Wang, D. Zhang, L. Sui, D. Ke, S. Li, Y. Jiang and M. Jin, *Phys. Plasmas*, 2017, **24**, 103305.
15 Y. Lu, Y. S. Zhou, W. Qiu, X. Huang, L. Liu, L. Jiang, J. F. Silvain and Y. F. Lu, *J. Anal. At. Spectrom.*, 2015, **30**, 2303–2306.
16 P. K. Pandey and R. K. Thareja, *Phys. Plasmas*, 2013, **20**, 022117.
17 S. Eschlböck-Fuchs, M. J. Haslinger, A. Hinterreiter, P. Kolmhofer, N. Huber, R. Rössler, J. Heitz and J. D. Pedarnig, *Spectrochim. Acta, Part B*, 2013, **87**, 36–42.
18 R. Sanginés, H. Sobral and E. Alvarez-Zauco, *Spectrochim. Acta, Part B*, 2012, **68**, 40–45.
19 Y. Wang, A. Chen, Y. Jiang, L. Sui, X. Wang, D. Zhang, D. Tian, S. Li and M. Jin, *Phys. Plasmas*, 2017, **24**, 013301.
20 R. Sanginés, H. Sobral and E. Alvarez-Zauco, *Appl. Phys. B: Lasers Opt.*, 2012, **108**, 867–873.
21 L. Liu, S. Li, X. N. He, X. Huang, C. F. Zhang, L. S. Fan, M. X. Wang, Y. S. Zhou, K. Chen, L. Jiang, J. F. Silvain and Y. F. Lu, *Opt. Express*, 2014, **22**, 7686–7693.
22 L. Liu, X. Huang, S. Li, Y. Lu, K. Chen, L. Jiang, J. F. Silvain and Y. F. Lu, *Opt. Express*, 2015, **23**, 15047–15056.
23 C. Goueguel, S. Laville, F. Vidal, M. Sabsabi and M. Chaker, *J. Anal. At. Spectrom.*, 2010, **25**, 635–644.
24 S. Lui and N. Cheung, *Anal. Chem.*, 2005, **77**, 2617–2623.
25 A. De Giacomo, R. Gaudiuso, C. Koral, M. Dell'Aglio and O. De Pascale, *Anal. Chem.*, 2013, **85**, 10180–10187.
26 A. Chen, Y. Jiang, T. Wang, J. Shao and M. Jin, *Phys. Plasmas*, 2015, **22**, 033301.
27 J. Shen, Z. Yang, X. Liu, Y. Shi, P. Zhao, S. Sun and B. Hu, *Plasma Sci. Technol.*, 2014, **17**, 147.
28 D. X. Sun, M. G. Su, C. Z. Dong and G. H. Wen, *Plasma Sci. Technol.*, 2014, **16**, 374–379.

29 X. M. Lin, H. Li and Q. H. Yao, *Plasma Sci. Technol.*, 2015, **17**, 953–957.
30 Z. Hou, Z. Wang, J. Liu, W. Ni and Z. Li, *Opt. Express*, 2014, **22**, 12909–12914.
31 L. B. Guo, W. Hu, B. Y. Zhang, X. N. He, C. M. Li, Y. S. Zhou, Z. X. Cai, X. Y. Zeng and Y. F. Lu, *Opt. Express*, 2011, **19**, 14067–14075.
32 L. Guo, B. Zhang, X. He, C. Li, Y. Zhou, T. Wu, J. Park, X. Zeng and Y. Lu, *Opt. Express*, 2012, **20**, 1436–1443.
33 Z. Hao, L. Guo, C. Li, M. Shen, X. Zou, X. Li, Y. Lu and X. Zeng, *J. Anal. At. Spectrom.*, 2014, **29**, 2309–2314.
34 A. Hussain, X. Gao, Z. Hao and J. Lin, *Optik*, 2016, **127**, 10024–10030.
35 X. J. Su, W. D. Zhou and H. G. Qian, *J. Anal. At. Spectrom.*, 2014, **29**, 2356–2361.
36 A. A. I. Khalil, *Opt. Laser Technol.*, 2015, **75**, 105–114.
37 D. Zhang, A. Chen, X. Wang, Y. Wang, L. Sui, D. Ke, S. Li, Y. Jiang and M. Jin, *Spectrochim. Acta, Part B*, 2018, **143**, 71–77.
38 Y. Liu, Y. Tong, Y. Wang, D. Zhang, S. Li, Y. Jiang, A. Chen and M. Jin, *Plasma Sci. Technol.*, 2017, **19**, 125501.
39 Y. T. Fu, Z. Y. Hou and Z. Wang, *Opt. Express*, 2016, **24**, 3055–3066.
40 X. Li, Z. Yang, J. Wu, W. Wei, Y. Qiu, S. Jia and A. Qiu, *J. Phys. D: Appl. Phys.*, 2017, **50**, 015203.
41 Y. Wang, H. Yuan, Y. Fu and Z. Wang, *Spectrochim. Acta, Part B*, 2016, **126**, 44–52.
42 S. H. Tavassoli and A. Gragossian, *Opt. Laser Technol.*, 2009, **41**, 481–485.
43 S. S. Harilal, G. V. Miloshevsky, P. K. Diwakar, N. L. LaHaye and A. Hassanein, *Phys. Plasmas*, 2012, **19**, 083504.
44 S. Amin, S. Bashir, S. Anjum, M. Akram, A. Hayat, S. Waheed, H. Iftikhar, A. Dawood and K. Mahmood, *Phys. Plasmas*, 2017, **24**, 083112.
45 Y. Wang, A. Chen, Q. Wang, L. Sui, D. Ke, S. Cao, S. Li, Y. Jiang and M. Jin, *Phys. Plasmas*, 2018, **25**, 033302.
46 Y. Tian, B. Xue, J. Song, Y. Lu, Y. Li and R. Zheng, *Appl. Phys. Express*, 2017, **10**, 072401.
47 Y. Wang, A. Chen, S. Li, D. Ke, X. Wang, D. Zhang, Y. Jiang and M. Jin, *AIP Adv.*, 2017, **7**, 095204.
48 S. U. Haq, L. Ahmat, M. Mumtaz, H. Shakeel, S. Mahmood and A. Nadeem, *Phys. Plasmas*, 2015, **22**, 083504.
49 T. T. P. Nguyen, R. Tanabe and Y. Ito, *Opt. Laser Technol.*, 2018, **100**, 21–26.
50 J. Tang, D. Zuo, T. Wu and Z. Cheng, *Opt. Commun.*, 2013, **289**, 114–118.
51 K. Matsui, T. Shimano, J. A. Ofosu, K. Komurasaki, T. Schoenherr and H. Koizumi, *Vacuum*, 2017, **136**, 171–176.
52 S. Zhang, S. Sheta, Z.-Y. Hou and Z. Wang, *Front. Phys.*, 2017, **13**, 135201.
53 Z. Y. Hou, Z. Wang, J. M. Liu, W. D. Ni and Z. Li, *Opt. Express*, 2013, **21**, 15974–15979.
54 X. Su, W. Zhou and H. Qian, *Opt. Express*, 2014, **22**, 28437–28442.